01 Jan 1993

A Study Of Fatigue Failure In Superalloys Using Positron Annihilation

D. Hoeckelman

Hollis P. Leighly
Missouri University of Science and Technology

Recommended Citation

D. Hoeckelman and H. P. Leighly, "A Study Of Fatigue Failure In Superalloys Using Positron Annihilation," *physica status solidi (a)*, vol. 138, no. 1, pp. 147 - 156, Wiley, Jan 1993.
The definitive version is available at https://doi.org/10.1002/pssa.2211380113

phys. stat. sol. (a) **138**, 147 (1993)

Subject classification: 62.20; 61.70; 78.70; S1.1; S1.2

Department of Metallurgical Engineering, University of Missouri-Rolla, Rolla[1])

A Study of Fatigue Failure in Superalloys Using Positron Annihilation

By

D. HOECKELMAN and H. P. LEIGHLY, JR.

This study shows there are significant changes occurring in the open volume defect concentration during fatigue cycling as measured by the S parameter. These changes are dependent upon the stress ratio, $R = \sigma_{min}/\sigma_{max}$, the maximum stress, σ_{max}, and the number of fatigue cycles. The decline in the S parameter is due to the elimination of the residual vacancies. This decline is followed by an increase due to the generation of dislocations and the formation of small microcracks. This is followed by a decline in the S parameter due to growth of the microcracks ultimately leading to failure.

Измерение S-параметра во время усталостного циклирования показало, что концентрация дефектов в открытом обьеме значительно меняется. Эти изменения зависят от отношения напрпяжений $R = \sigma_{min}/\sigma_{max}$, максимального напряжения σ_{max} и числа усталостных циклов. Значение S-параметра уменьшается в результате исчезновения остаточных вакансий. За этим уменьшением следует увеличение, которое можно объяснить образованием дислокаций и микротрещин. Затем значение S-параметра уменьшается в результате дальнейшего развития микротрещин, что в конечном счете приводит к разрушению.

1. Introduction

Fatigue cycling is known to cause microstructural damage to metals and alloys and to rearrange defect structures. Feltner and Laird [1] have shown that fatigue cycling will increase the yield strength of well-annealed copper due to the introduction of defects, while similar fatigue cycling of cold-worked copper reduces the tensile properties due to the elimination of some of the defects and the rearrangement of other defects into a more stable configuration. Sivashankaran and Welsch [2] showed in well-annealed nickel that the resistivity ratio increased with fatigue cycles. They determined that a large increase occurred in the first 500 cycles at 241 MPa due both to vacancy and dislocation generation. For more cycles, the contribution to the resistivity ratio from dislocations was fixed while the contribution from vacancies continued to increase. Suresh [3] has shown that there is a very large increase in the vacancy concentration resulting from fatigue cycling. Cheng and Laird [4] measured the number and sizes of the microcracks that developed as a function of the number of fatigue cycles. They found that the number of small cracks remained constant while the size and number of larger cracks increased indicating that the generation rate of small cracks is constant to replace those cracks that have grown.

Doppler broadening positron annihilation has been used extensively to study defects in metals and alloys (Hautojärvi [5]). From the positron–electron annihilation spectrum, the lineshape or S parameter is determined in the usual way (MacKenzie et al. [6]). Increasing the open volume defect concentration will cause an increase in the value of the S parameter.

[1]) 218 McNutt Hall, Rolla MO 65401, USA.

Coleman et al. [7] have measured an increase in the S parameter in a titanium alloy as a function of the number of fatigue cycles and position along the specimen axis after one cycle and 900 cycles. The S parameter increases with the number of cycles and with the increase in the stress amplitude. Hughes [8] found significant changes in the S parameter in the vicinity of a fatigue crack in 18/8 stainless steel. Near the crack tip, the S parameter is large indicating a high density of defects trapping positrons. Gauster et al. [9] found that the S parameter increases more rapidly during high strain amplitude cycles than during lower strain amplitude in SAE 316 stainless steel. An accompanying series of transmission electron graphs reveals a continuing increase in dislocation concentration with a reduced cell size in the grains with increasing fatigue cycling. Sharma et al. [10] determined the S parameter in the plastic zone of a fatigue-cracked fracture mechanics specimen. It had the largest value near the crack tip, declining as the distance from the crack tip increased.

Karjalainen et al. [11] performed a bend fatigue experiment using OFHC copper sheet specimens 4 mm thick which had been annealed prior to fatigue testing at 873 K for 30 min followed by air cooling. Their results showed that the S parameter for the annealed specimens increased after a few fatigue cycles. After these initial cycles, there was a very substantial decrease in the S parameter versus fatigue cycle curves to a minimum in both of the annealed specimens. Additional fatigue cycles cause a subsequent increase in the S parameter. The number of cycles to cause development of the minimum was dependent upon the strain amplitude; the larger the strain amplitude, the fewer the number of the fatigue cycles needed to develop the minimum.

2. Experimental Procedure

2.1 Experimental materials

For this experiment, two commercial superalloys were used: Inconel 718 and Incoloy 903. The composition of these alloys is given in Table 1. The vendor of these alloys prior to delivery heated them into the solid solution temperature range followed by quenching in water to provide a supersaturated solid solution. The alloys were machined into tensile

Table 1
Composition of the superalloys (in %)

composition	Inconel 718	Incoloy 903
Ni	50–55	38
Cr	17–21	21–23
Nb	4.75–5.5	3.0
Mo	2.8–3.3	
Ti	0.65–1.15	1.4
Al	0.2–0.8	0.9
Co	1.0 max	15
C	0.08 max	
Mn	0.35 max	
Si	0.35 max	
P	0.015 max	
S	0.015 max	
B	0.006 max	
Cu	0.3 max	
Fe	balance	

Table 2
Heat treatment of superalloys

solution heat treatment	
Inconel 718 1 h 1253 K water quench	Incoloy 903 1 h, 1253 K water quench
precipitation hardening heat treatment	
8 h, 991 K furnace cool to 894 K, hold for a total time of 18 h air cool	8 h, 991 K furnace cool to 894 K, hold for a total time of 16 h air cool
precipitates	
γ', $Ni_3(Al, Ti)$, $L1_2$	γ'', Ni_3Nb, ordered b.c.t.

fatigue specimens having threaded ends and a reduced section 31 mm long and 6 mm in diameter. After machining, the specimens were given the recommended precipitation heat treatment to produce the as-aged condition. The heat treatments for these alloys is given in Table 2. The strengthening mechanism in both alloys is the result of precipitate formation during heat treatment, γ' in Inconel 718 and γ'' Incoloy 903.

2.2 *Fatigue testing*

The axial fatigue testing was done using an MTS servocontrolled mechanical testing machine having a 8.9×10^4 N capacity. In this experiment, the fatique stress was controlled. The axial fatigue test frequency used was 8 cycles/s. After a selected number of cycles, the specimen was removed from the testing machine for the positron annihilation measurements. After the positron measurement, the specimen was reinserted into the testing machine. For these fatigue tests, two stress ratios, $R = \sigma_{min}/\sigma_{max}$, where σ_{max} and σ_{min} are the maximum and minimum stress, were used; $R = 0$ and 0.5.

2.3 *Doppler broadening positron annihilation*

The specimen support apparatus for Doppler broadening positron annihilation is constructed following an existing design (Coleman et al. [12]). Each specimen was positioned for Doppler broadening measurement having the same relationship to the positron source and the detector. The fatigue specimen is supported in a beam of positrons emitted from an encapsulated ^{22}NaCl positron source. A Ge(Li) detector receives the annihilation γ-rays. The positron source and the detector are arranged so that the detector does not receive any positrons. The energy of each photon is determined by the detector and stored in the appropriate energy channel of a multichannel analyzer. Data are collected for 2000 s so that about 10^6 annihilation γ-ray photons are recorded to yield a spectrum. The S parameter is determined in the usual way (MacKenzie et al. [6]) from the annihilation γ-ray spectrum. The error in the S parameter values is $\approx$0.1%.

3. Experimental Results

3.1 Inconel 718

The selected stress amplitude for all the fatigue tests is large enough to cause fatigue failure to occur if the specimen is subjected to enough fatigue cycles. This is done so that the S parameter would measure changes in the defect concentration as fatigue damage progresses toward failure. The S parameter is determined for the specimen in the as-aged condition and after a selected number of fatigue cycles. The S parameter data as a function of the number of fatigue cycles has been normalized to the S parameter for the as-aged condition which is shown at the left end of the abscissa scale in all of the figures. In Fig. 1, the normalized S parameter is plotted versus the number of axial fatigue cycles for Inconel 718 when $R = 0.5$ and σ_{max} is equal to 1021, 915, and 633 MPa. It is apparent that 2000 fatigue cycles at $\sigma_{max} = 915$ MPa reduces the S parameter substantially, indicating a significant reduction in the positron trapping concentration. When σ_{max} is 633 MPa, it is evident that the deep minimum seen previously would have appeared if the number of stress cycles had been greater than 2000 and less than 5000 while the specimen subjected to fatigue cycling at $\sigma_{max} = 1021$ MPa would have had a minimum at less than 2000 cycles. This assumes that the deep minima are characteristic of the S parameter versus fatigue data.

There is a subsequent increase in the S parameter peaking at 10000 cycles after the initial decline followed by a final decline. Refer to Fig. 2 which consists of the data already shown in Fig. 1 plus the data for three other values of σ_{max}. When $\sigma_{max} = 1161$ and 774 MPa, S parameters show similar behavior to that shown in Fig. 1. The depths of the minima are not as great as in the case of $\sigma_{max} = 915$ MPa. For specimens using $\sigma_{max} > 915$ MPa, the deepest minimum would have been at fewer than 2000 cycles while, for $\sigma_{max} < 915$ MPa the deepest minimum would be at greater than 2000 cycles. In the case where $\sigma_{max} = 1190$ MPa,

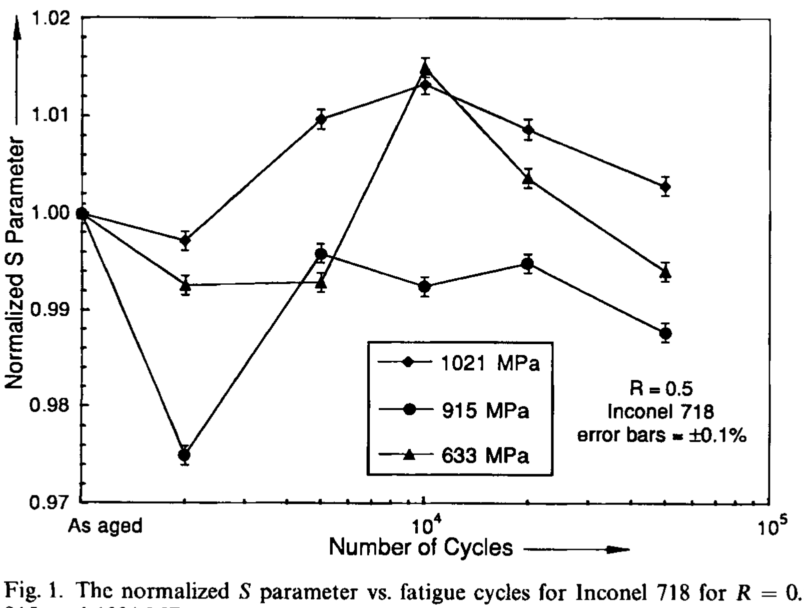

Fig. 1. The normalized S parameter vs. fatigue cycles for Inconel 718 for $R = 0.5$ while $\sigma_{max} = 633$, 915, and 1021 MPa

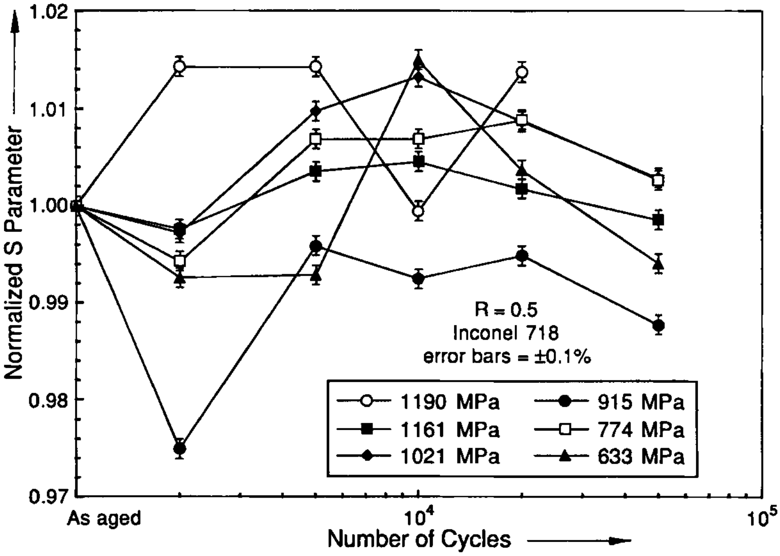

Fig. 2. The normalized S parameter vs. fatigue cycles for Inconel 718 when $R = 0.5$

the minimum occurs at so few cycles that it has no effect on the S parameter at 2000 cycles.

After the initial minimum, the S parameter in Fig. 2 peaks at about 10000 cycles except when $\sigma_{max} = 1190$ MPa. This indicates an increase in the concentration of the positron traps. For a further increase in the number of cycles, there is a decline from the peak value due to a loss of positron traps. When $\sigma_{max} = 1190$ MPa, the decline normally observed at

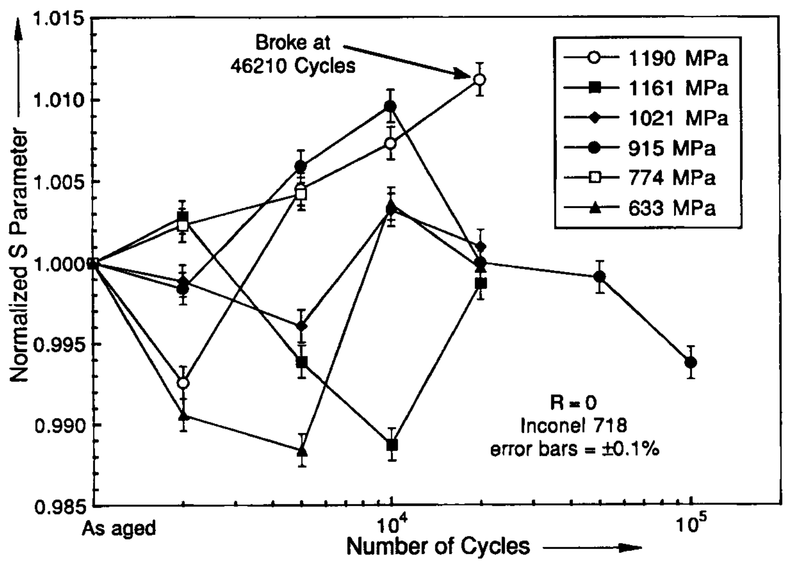

Fig. 3. The normalized S parameter vs. fatigue cycles for Inconel 718 when $R = 0$

50000 cycles is shifted to 10000 cycles. This is the result of the rapid loss of positron traps at this high stress level. Except for the highest and the lowest values of σ_{max}, the behavior of the S parameter versus fatigue cycles is quite similar.

In Fig. 3, the results are somewhat different from those in Fig. 2 due to the difference in the stress ratio, i.e., $R = 0$. The reduction in the value of R causes an increase in the damage to the microstructure by the fatigue cycling. Dieter [13] has presented a graph showing a reduction in the fatigue limit as the value of R is reduced. The initial minima have been reduced to much smaller numbers of fatigue cycles due to the increased fatigue damage. In fact, for certain stresses there are no minima in the graph because they may have occurred at so few fatigue cycles that they had no effect on the S parameter at 2000 cycles. In the case in which $\sigma_{max} = 1190$ MPa, it appears that the minimum at 10000 cycles shown in Fig. 2 has been shifted to produce a minimum at 2000 cycles. When $\sigma_{max} = 1161$ MPa, the initial decline at 2000 cycles is completely lost, giving at 2000 cycles some portion of the peak that in Fig. 2 was at 5000 cycles. In general, there is a strong shift of the features shown in Fig. 2 to fewer cycles in Fig. 3 due to the change in the stress ratio causing more damage to the microstructure.

3.2 Incoloy 903

Incoloy 903 has a lower yield strength (1140 MPa) as compared with Inconel 718, in which the yield strength is 1240 MPa. In addition, the precipitate particles formed during the precipitation hardening in Inconel 718 are γ' while in Incoloy 903, there are γ''. These two factors will result in some differences in the value of the S parameter versus fatigue cycles in addition to the similarities.

Comparing Fig. 4 with Fig. 1 and 2, the minima and the peaks are similar in that they occur at about the same number of fatigue cycles. When $\sigma_{max} = 703$ MPa and 1091 MPa, the values for the S parameter at 2000 cycles are almost the same. The true minimum would

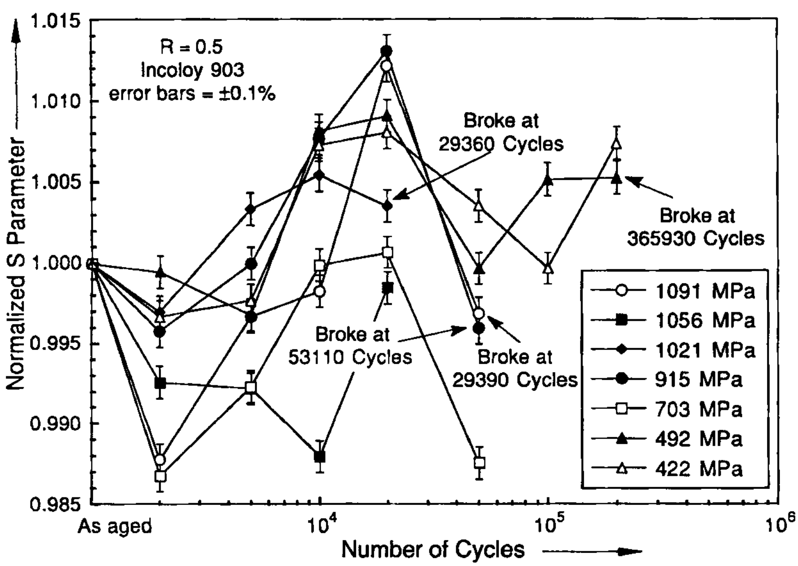

Fig. 4. The normalized S parameter vs. fatigue cycles for Incoloy 903 when $R = 0.5$

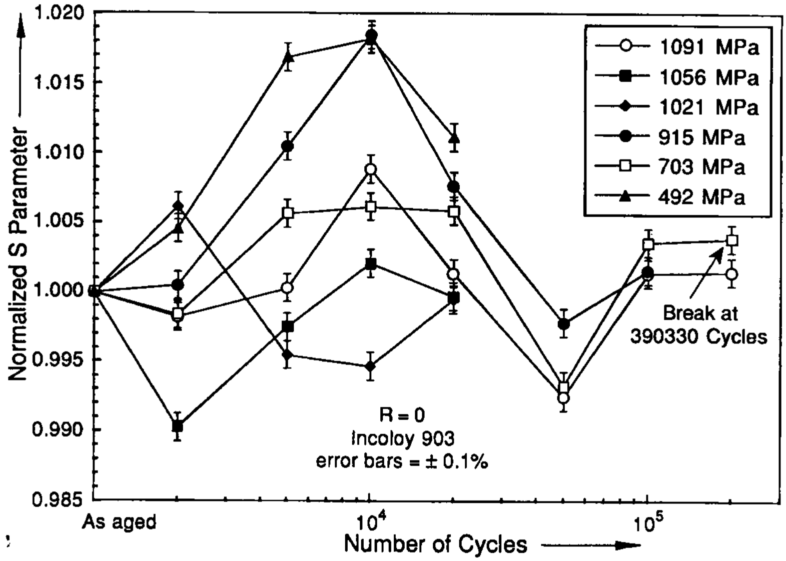

Fig. 5. The normalized S parameter vs. fatigue cycles for Incoloy 903 when $R = 0$

have been at less than 2000 cycles when $\sigma_{max} = 1091$ MPa while, for $\sigma_{max} = 703$ MPa, the true minimum should have been between 2000 and 5000 cycles. The true minima for the other specimens should have correspondingly different numbers of fatigue cycles. In general, the data for Incoloy 903 have a minimum at 2000 cycles with a peak occurring at 20000 cycles followed by a decline, similar to the data presented in Fig. 2. The S parameters for the specimens subjected to fatigue cycling when $\sigma_{max} = 492$ and 422 MPa are almost the same throughout the range of the experiment, as should be expected.

In Fig. 5, when $R = 0$, the rate of damage is more severe than for the data shown in Fig. 4. The features have been shifted to fewer cycles. The true minima for several stress levels occur at so few cycles that there is little or no effect on the S parameter at 2000 cycles. It is often lost. The peak of the S parameter for the various specimens has been shifted to 10000 cycles from 20000 cycles, as shown in Fig. 4. The second minima in both figures occur in 50000 cycles. In both figures, there is a small increase in the S parameter after the second minima.

4. Discussion of Results

An examination of the S parameter versus cycles curves presented in Fig. 1 to 5 shows a similar pattern of behavior for all specimens with some easily explained differences. Specifically, there are significant minima in the curve of S parameter versus fatigue cycles after a fairly small number of fatigue cycles. Because the number of stress cycles selected for the first fatigue increment is fixed at 2000 cycles for the axial fatigue tests, the depths of the minima are dependent on the stress amplitude. When very large stress amplitudes are used, or when $R = 0$, the minima will have occurred after fewer cycles, hence they may be obscured by the subsequent fatigue damage to the specimen. Similarly, using low fatigue stress levels causes the minima to appear at a larger number of cycles (> 2000 cycles), again

not to be observed because of the number of the fatigue cycles selected for tests to determine the S parameter.

To understand this reduction in the S parameter, it must be recognized that defects such as vacancies, grain boundaries, and dislocations can act as traps for positrons. In Doppler broadening positron annihilation, the presence of defects alters the annihilation γ-ray spectrum increasing the S parameter (MacKenzie et al. [6]). The decrease observed in the S parameter indicates a reduction in the trapping concentration. The alloys used in this experiment, Inconel 718 and Incoloy 903, were received from the vendor in the solution heat treated and water quenched condition as shown in Table 2. This treatment and subsequent mechanical and thermal treatments will not have affected the total area of the grain boundaries, thus the S parameter changes could not have been the result of any grain growth. The dislocation density in the alloys should have been small in the as-received alloy due to the solution heat treatment at 1253 K. The precipitation hardening treatment at 894 K given after machining should have removed any dislocation introduced by this procedure.

The specimens were air cooled from 894 K after the precipitation hardening heat treatment. The small diameter of the fatigue specimen, 6 mm, the rapid cooling rate, and the high alloy content with its accompanying vacancy–impurity binding energy will have been fast enough to retain some of the vacancies and vacancy clusters that were present at equilibrium at 894 K. The retained vacancies and vacancy clusters will trap positrons increasing the S parameter. The decline in the S parameter during the first few fatigue cycles must be the result of an alteration in the vacancy concentration and configuration.

Any residual dislocation present after the precipitation hardening heat treatment may oscillate during fatigue around some quasi-equilibrium position in the lattice to capture in vacancies and vacancy clusters, reducing their concentration and reducing the S parameter. The larger the fatigue stress, the greater the mobile dislocation concentration, the larger their amplitude, and the faster is the removal of the excess vacancies. This will also accelerate the reduction in the S parameter. The extent of the difference of the value of the S parameter between the aged condition and after 2000 fatigue cycles is the result of the large loss of defects or substantial clustering.

After elimination or clustering of the residual vacancies by the initial fatigue cycling, the S parameter begins to rise. Gauster et al. [9] and Mughrabi et al. [14] have presented transmission electron microscope micrographs in which the dislocation concentration is seen to increase with increasing fatigue cycles. This parallels the increase in the S parameter. It should not be assumed that dislocation formation must await the elimination of all of the excess vacancies. In the early fatigue stages, the excess vacancies and their removal dominate the S parameter versus fatigue cycle leading to the minima. It is evident that dislocations have become the dominant positron traps as the S parameter reaches a peak before a subsequent decline. This peak represents a saturation of the lattice with positron traps. Karjalainen et al. [11] observed a similar behavior in air cooled copper where they observed a small increase in the S parameter followed by a significant decrease with increasing fatigue cycles. With still more fatigue cycles, the decline was reversed.

Ma and Laird [15] and Neumann and Tönnessen [16] showed the initiation of microcracks during fatigue in conjunction with the development of persistent slip bands (PBS). Cheng and Laird [4] have shown that the number and size of the microcracks increases with fatigue cycles. When the microcracks are very small, positrons will be trapped as if the microcracks were small voids. Hautojärvi et al. [17] have found that voids are able to trap positrons.

This ability is dependent upon the void size. The S parameter initially increases with an increase in void size but the rate of increase in the S parameter then declines with increasing void size. The size dependence of the S parameter vanishes when the voids reach a diameter of 1.2 nm due to a vanishing of the electron density in the void. Non-local correlation effects become important in large voids and an image-potential-induced surface state becomes energetically favorable. If the microcracks are small enough, they will act as voids in trapping positrons increasing the S parameter. The microcracks will have an ellipsoid shape with a large dimension normal to the stress axis and a small dimension parallel to it. As they grow normal to the stress axis, the distance between the surfaces in the center of the microcracks will exceed the limit of 1.2 nm. When this happens, only those surfaces around the perimeter of the microcracks will be close enough to trap positrons. Initially, the total perimeter region in the many microcracks will be large, hence there will be little effect on the S parameter. However as the microcracks grow and agglomerate, the total amount of crack perimeter capable of acting as positron traps becomes smaller. This will be reflected by the decline in the S parameter. This microcrack growth will contribute to the negative slope of the S parameter versus fatigue cycle curve.

5. Conclusions

The observed changes in the S parameter versus fatigue cycles has been explained in terms of the defect concentration, the stress ratio, R, the stress maximum, σ_{max}, and the number of fatigue cycles. The initial decline in the curve is due to the removal of residual vacancies followed by an increase due to an increase in dislocations and microcracks. The final decline should be the result to the growth and agglomeration of the microcracks.

Acknowledgements

The financial support provided by NASA is gratefully acknowledged. The authors wish to thank Prof. R. W. Stephenson, Prof. A. E. Bolon, and the staff of the UMR reactor for assistance in performing the experiment and to Prof. Jay Gregg for his assistance in preparing this paper.

References

[1] C. E. Feltner and C. Laird, Acta metall. **15**, 1621 (1967).
[2] S. Sivashankaran and G. Welsch, Proc. 9th Canad. Fracture Conf., Canad. Met. Quarterly, 1981.
[3] S. Suresh, Fatigue 90, Ed. H. Kitagawa and T. Tanaka, Materials and Components Engineering Publications, Birmingham (UK) 1990 (p. 759).
[4] A. S. Cheng and C. Laird, Fatigue Engng. Mater. Structure **4**, 331 (1981).
[5] P. Hautojärvi, Positron Annihilation in Solids, Topics in Current Physics, Vol. 12, Springer-Verlag, Berlin 1979 (p. 89).
[6] I. K. MacKenzie, J. A. Eady, and R. R. Gingrich, Phys. Letters A **33**, 279 (1970).
[7] C. F. Coleman, A. E. Hughes, F. A. Smith, and M. J. Weaver, NDT Internat. **15**, 87 (1982).
[8] A. E. Hughes, Mater. Engng. **2**, 34 (1980).
[9] W. B. Gauster, W. R. Wampler, W. R. Jones, and J. A. van den Avyle, SAND77-1570, R-7, Sandia Nat. Lab., Albuquerque (N.M.) 1978.
[10] S. C. Sharma, R. M. Jones, and L. M. Dean, Proc. ASM-AIME Meeting, Novel NDE Methods for Materials, Dallas, Ed. B. B. Rath, The Metallurgical Society, Pittsburgh 1982 (p. 45).

[11] L. P. Karjalainen, T. Juden, and M. Karras, Positron Annihilation, Ed. P. G. Coleman, S. C. Sharma, and L. M. Diana, North-Holland Publ. Co., New York 1982 (p. 461).
[12] C. F. Coleman, F. A. Smith, and A. E. Hughes, AERE-R8551, Atomic Energy Research Establishment, Harwell 1979.
[13] G. E. Dieter, Mechanical Metallurgy, 3rd ed., McGraw-Hill Book Co., New York 1986 (p. 383).
[14] H. Mughrabi, F. Ackermann, and K. Herz, Fatigue Mechanisms, STP 675, Amer. Soc. Testing and Materials, Philadelphia 1979 (p. 69).
[15] B.-T. Ma and C. Laird, Acta metall. **37**, 325 (1989).
[16] P. Neumann and A. Tönnessen, Proc. 2nd Engineering Conf./Workshop, Small Fatigue Cracks, Santa Barbara, Ed. R. O. Ritchie and J. Lankford, The Metallurgical Society, Pittsburgh 1986 (p. 41).
[17] P. Hautojärvi, T. Heinio, and M. Manninen, Phil. Mag. **35**, 973 (1977).

(Received March 12, 1993)